



Influence of Annealing Temperature on the Microstructure and Mechanical Properties of T4003 Ferritic Stainless Steel for Pipe Organ Rail Rod Components

Wen Sun ^{1,*}

<https://doi.org/10.64486/m.65.3.2>

¹ Harbin University, No. 109 Zhongxing Avenue, Nangang District, Harbin City, Heilongjiang Province, China, 150086; sunwen@lsu.edu.gn

* Correspondence: sunwen@lsu.edu.gn

Type of the Paper: Article

Received: September 4, 2025

Accepted: December 19, 2025

Abstract: T4003 ferritic stainless steel is a high-strength spring steel with excellent elasticity, toughness, and corrosion resistance, making it suitable for precision components such as pipe organ rail rod mechanisms. This study systematically investigates the influence of annealing temperature (640–850) °C on the microstructure and mechanical properties of T4003 steel. Microstructural characterization was performed using optical microscopy, while mechanical properties including yield strength, tensile strength, section shrinkage, and yield-to-tensile ratio were evaluated. The results indicate that annealing at 850 °C promotes complete recrystallization and the formation of a fine, homogeneous ferritic grain structure, leading to optimal mechanical performance with a yield strength of 508 MPa and tensile strength of 614 MPa. However, a strength-ductility trade-off was observed, with ductility peaking at intermediate temperatures. The findings provide practical guidance for the heat treatment of T4003 steel in high-precision mechanical applications.

Keywords: pipe organ rail rod mechanism; T4003 stainless steel; microstructure; mechanical properties

1. Introduction

Pipe organs represent one of the most mechanically complex and acoustically nuanced musical instruments, wherein the precise transfer of motion from the keyboard to the air valves governing individual pipes is critical to tonal clarity, responsiveness, and reliability. Central to this transfer system is the rail rod mechanism, an assembly of linked rods, levers, and rollers that converts the downward force of a key into the vertical lift of a pallet valve, allowing pressurized air to enter a specific pipe. Given that a large organ may contain thousands of such components, each subjected to repetitive cyclic loading during performance, the material selection for rail rods directly influences the instrument's tactile feedback, longevity, and maintenance frequency.

Traditional materials such as plain carbon steels or brass may suffer from fatigue, corrosion in humid environments, or excessive elastic deformation, leading to sluggish response or eventual failure. Consequently, there is a growing interest in high-performance stainless steels that offer a blend of strength, corrosion resistance, and dimensional stability. T4003 ferritic stainless steel has emerged as a promising candidate owing to its high

yield strength, excellent atmospheric corrosion resistance, and good manufacturability—attributes that align well with the demanding service conditions of pipe organ rail rod mechanisms [1-3].

T4003 belongs to the family of high-strength ferritic stainless steels, typically strengthened through solid-solution hardening, grain refinement, and precipitation of micro-alloying elements such as Nb and Ti [4-7]. Its low carbon content minimizes sensitization and improves weldability, which is advantageous for assembling complex rod-linkage systems [8-10]. Previous studies have highlighted the steel's utility in railway vehicles and structural springs, yet its adaptation to precision musical-instrument mechanisms remains underexplored. In particular, the effect of post-fabrication heat treatment specifically annealing temperature on the microstructural and mechanical properties of T4003 in the context of rail rod performance has not been systematically addressed [11-13].

Annealing is a critical step in tailoring the microstructure of cold-worked or cast stainless steel components. For ferritic grades like T4003, annealing in the range of 640–850 °C can induce recovery [14], recrystallization [15], and phase transformations [16], each of which profoundly affects strength, ductility, and elastic modulus [17]. While general annealing behavior of ferritic stainless steels is documented, a detailed investigation linking temperature-driven microstructural changes to the specific mechanical requirements of pipe organ rail rods high stiffness to maintain action precision, sufficient ductility to withstand occasional over-loads, and corrosion resistance to ensure decades of service is lacking [18-20].

This study therefore aims to systematically examine the influence of annealing temperature (640, 680, 730, 780, 830, and 850) °C on the microstructure and mechanical properties of T4003 ferritic stainless steel. We hypothesize that an optimal annealing temperature exists that produces a fine, homogeneous ferritic grain structure through complete recrystallization, thereby achieving an optimal balance between static strength, elastic limit, and ductility. The findings are expected to provide scientifically grounded heat-treatment guidelines for manufacturing high-reliability rail rod components and, by extension, contribute to the material-selection framework for other precision mechanical systems requiring similar property profiles.

2. Materials and Methods

T4003 stainless steel was prepared by medium-frequency induction melting followed by sand casting. The chemical composition (mass fraction) is as follows: C: 0.015 %, Si: 0.43 %, Mn: 1.87 %, S: 0.001 %, P: 0.014 %, Cr: 11.68 %, Ni: 0.81 %, Nb: 0.08 %, Ti: 0.13 %, N: 0.014 %, Fe: balance.

Rectangular specimens were cut from the cast ingot and subjected to annealing in a box-type resistance furnace at temperatures of 640 °C, 680 °C, 730 °C, 780 °C, 830 °C, and 850 °C. Each specimen was held at the target temperature for 5 h, then quenched in water. Subsequently, the quenched samples were tempered at 450 °C for 2 h and again water-cooled to room temperature.

For microstructural examination, specimens were mounted, ground, polished, and etched with 3 % nitric acid in ethanol. Observations were carried out using a Nikon Eclipse LV100ND optical microscope. Scale bars were inserted on all micrographs to indicate the actual size of the features; the original “40×” magnification label was removed in accordance with editorial guidance.

Tensile tests were conducted on a SANS 5105 microcomputer-controlled electronic universal testing machine, following ASTM E8 standards. For each annealing condition, three specimens were tested to ensure statistical reliability. The standard deviation of the measured mechanical properties was calculated.

3. Results

Figure 1 illustrates the microstructural changes induced by different annealing temperatures. At 640 °C, the initial martensitic and ferritic constituents undergo recovery, leading to a reduction in elongated grains but also to noticeable grain-size inhomogeneity. Between 680 °C and 780 °C, the microstructure appears mixed, containing both ferrite and austenite (or transformed products), reflecting the material's passage through a two-phase region. When the temperature reaches (830–850) °C, the steel enters the fully austenitic phase field.

Upon subsequent cooling, the $\gamma \rightarrow \alpha$ transformation yields a fine, uniform ferritic grain structure, significantly reducing grain-size variability.

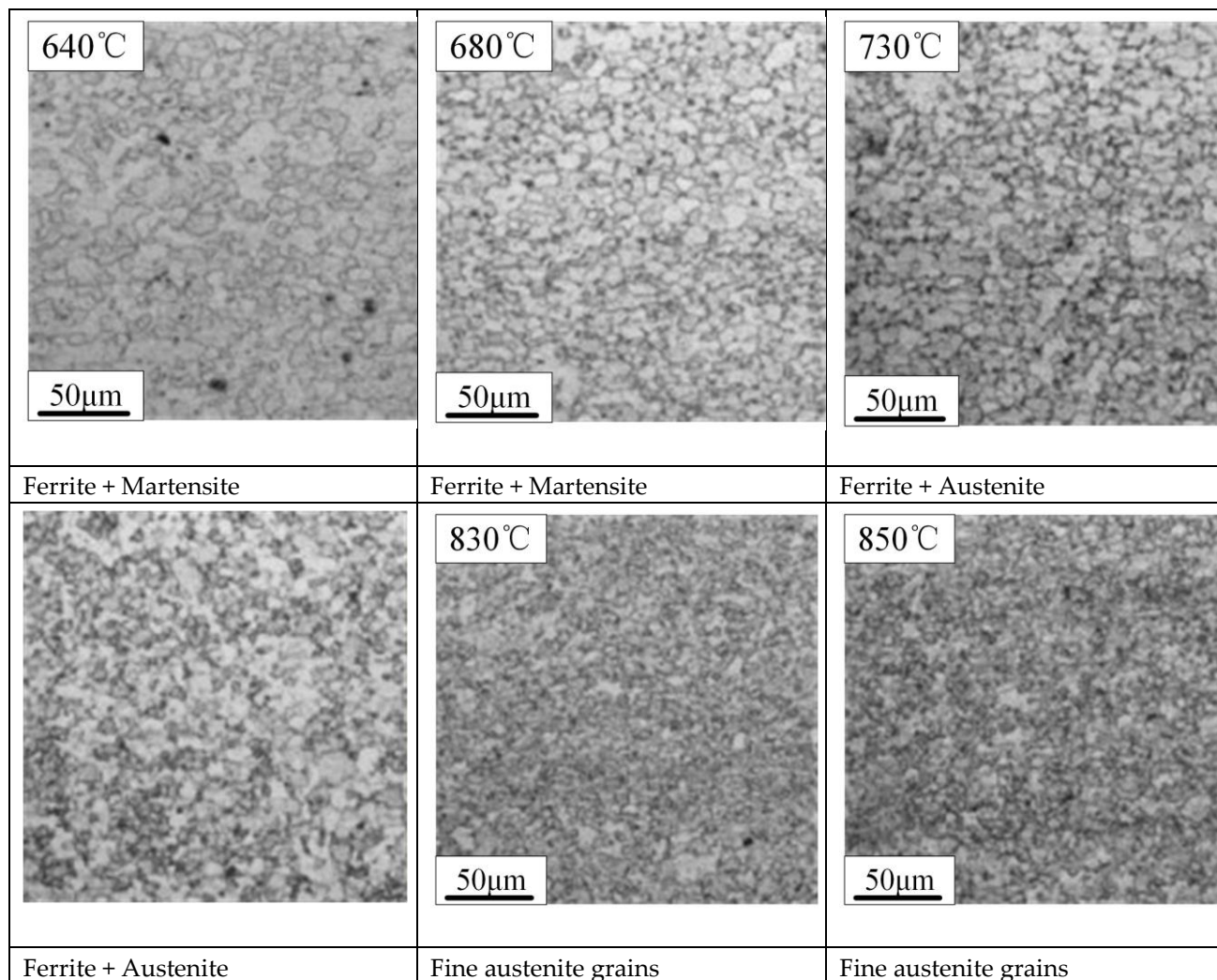


Figure 1. Effect of annealing temperature on the microstructure of the experimental steel

Mechanical properties as a function of annealing temperature are summarized in Table 1. The calculated sample standard deviations (based on three tests per condition) are included in parentheses; all values fell within ± 1.21 , confirming good experimental repeatability.

Table 1. Mechanical properties of the experimental steel at different annealing temperatures

| Number | Temperature °C | Yield strength MPa | Tensile strength/MPa | Section shrinkage % | Yield to tensile ratio/% |
|--------|-------------------|-----------------------|-------------------------|------------------------|-----------------------------|
| 1 | 640 | 475 ± 1.1 | 604 ± 0.9 | 29.4 ± 0.8 | 0.78 ± 0.01 |
| 2 | 680 | 349 ± 1.2 | 531 ± 1.1 | 30.7 ± 0.7 | 0.66 ± 0.02 |
| 3 | 730 | 371 ± 1.0 | 544 ± 1.0 | 26.4 ± 0.9 | 0.68 ± 0.01 |
| 4 | 780 | 448 ± 0.9 | 569 ± 1.2 | 24.8 ± 1.0 | 0.79 ± 0.02 |
| 5 | 830 | 461 ± 1.7 | 583 ± 0.8 | 24.3 ± 0.9 | 0.79 ± 0.01 |
| 6 | 850 | 508 ± 0.8 | 614 ± 0.9 | 23.1 ± 1.1 | 0.82 ± 0.01 |

The variation in yield strength of T4003 experimental steel with annealing temperature, as depicted in Figure 2, reflects the underlying microstructural evolution governed by thermal activation. The initial decrease

in yield strength within the lower temperature range (640–730) °C is indicative of the recovery process, during which dislocation annihilation and rearrangement reduce internal stresses and defect density, thereby softening the material. As the temperature increases further, partial recrystallization occurs but remains incomplete, resulting in a mixed and non-uniform grain structure that compromises strengthening consistency.

With annealing temperatures elevated to (780–850) °C, complete recrystallization takes place, followed by progressive grain growth. The notable increase in yield strength, reaching a maximum of 508 MPa at 850 °C, is principally attributed to grain refinement. This behavior aligns with the Hall–Petch relationship, wherein a reduction in grain size enhances the density of grain boundaries, effectively impeding dislocation glide and improving strength. At 850 °C, the steel resides entirely within the austenitic phase region. Subsequent cooling induces the $\gamma \rightarrow \alpha$ phase transformation, facilitating the development of a fine and uniform ferritic matrix. This structurally homogeneous and refined condition not only elevates yield strength but also promotes uniform plastic deformation, essential for structural reliability in service.

Figure 2 presents the variation of tensile strength in T4003 experimental steel as a function of annealing temperature, showing a characteristic non-monotonic trend that reflects the underlying microstructural evolution. At lower annealing temperatures (640–730) °C, the observed decrease in tensile strength is attributed to recovery processes and partial recrystallization, which reduce dislocation density and diminish strain-induced strengthening contributions. As the temperature rises to (780–850) °C, complete recrystallization occurs and is followed by grain refinement, leading to a significant strength recovery that peaks at 614 MPa at 850 °C. This enhancement is primarily due to grain boundary strengthening via the Hall-Petch mechanism, combined with the formation of a homogeneous fine-grained ferritic structure through the $\gamma \rightarrow \alpha$ phase transformation during cooling from the fully austenitic state, which collectively improve both strength and strain distribution during tensile deformation.

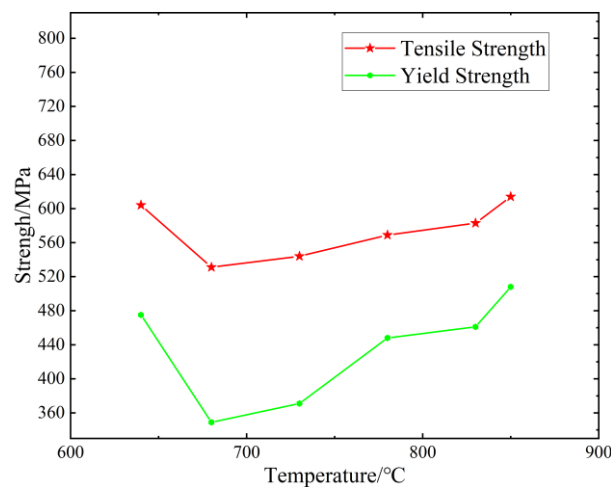


Figure 2. Effect of annealing temperature on yield strength and tensile strength of experimental steel

The variation of section shrinkage with annealing temperature, as shown in Figure 3, reveals a distinct trend that correlates directly with the microstructural evolution of T4003 steel. The section shrinkage initially increases to a maximum of 30.7 % at 680 °C, then progressively decreases at higher temperatures. This pattern reflects the competing effects between dislocation recovery and grain refinement on the material's plastic deformation capability.

At intermediate temperatures around 680 °C, adequate recovery of dislocation structures combined with incomplete recrystallization preserves substantial work hardening capacity while reducing stress concentrations, thereby maximizing ductility. However, as annealing temperatures increase beyond 730 °C, complete recrystallization and subsequent grain refinement occur, leading to a greater density of grain boundaries that simultaneously enhance strength but constrain coordinated plastic flow.

The finer grain structure developed at (830–850) °C, though beneficial for strength, limits dislocation mobility and reduces the material's capacity for uniform plastic deformation, resulting in diminished section

shrinkage. This inverse relationship between strength and ductility exemplifies the classic strength-ductility tradeoff in metallic materials, where the microstructural features that improve strength inevitably compromise plastic deformation capability.

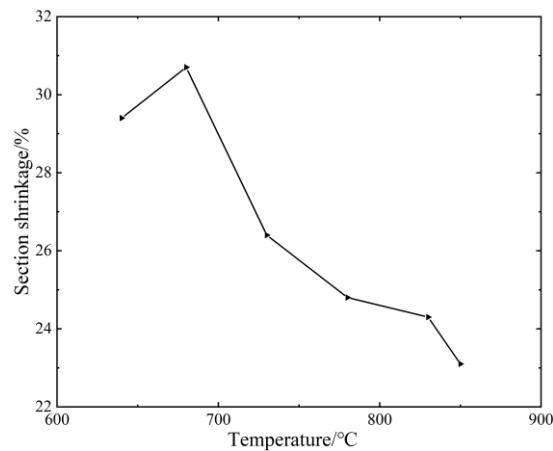


Figure 3. Effect of annealing temperature on section shrinkage of the experimental steel

The yield-to-tensile ratio (Y/T ratio) of T4003 steel exhibits a significant dependence on annealing temperature, as illustrated in Figure 4, increasing from 0.66 at 680 °C to 0.82 at 850 °C. This progressive elevation in Y/T ratio reflects a fundamental transition in the material's deformation behavior and microstructural state. At lower annealing temperatures (640-730) °C, the relatively lower Y/T ratio indicates enhanced strain hardening capability and improved plastic deformation uniformity, attributable to the presence of recovered but incompletely recrystallized structures that facilitate sustained work hardening.

As the annealing temperature increases to (780-850) °C, complete recrystallization and grain refinement lead to a marked increase in Y/T ratio, reaching 0.82 at 850 °C. This elevated ratio signifies a reduction in the material's work hardening capacity and a narrower plastic deformation range, characteristic of fine-grained microstructures where the increased grain boundary density restricts dislocation motion and promotes more uniform but limited plastic flow. The high Y/T ratio of 0.82 at 850 °C indicates superior dimensional stability under load and enhanced resistance to plastic deformation, making the material particularly suitable for applications requiring high structural stability and precise load-bearing characteristics, though with reduced capacity for plastic energy absorption.

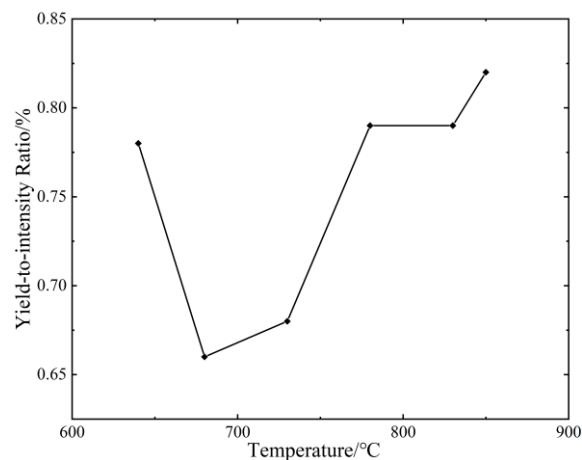


Figure 4. Effect of annealing temperature on yield-to-tensile ratio of the experimental steel

4. Discussion

The microstructural evolution observed in this study is consistent with the phase behavior of ferritic stainless steels. At lower annealing temperatures (640–780), the material lies within a two-phase ($\alpha+\gamma$) region, leading to incomplete recrystallization and a heterogeneous mixture of recovered martensite, ferrite, and retained austenite. This heterogeneity explains the relatively lower and more variable mechanical properties in this range. As the temperature exceeds ~ 800 °C, the steel becomes fully austenitic. During subsequent cooling, the $\gamma \rightarrow \alpha$ transformation proceeds via a diffusion-controlled process, resulting in a fine, equiaxed ferritic matrix. The refinement of the grain structure follows the Hall–Petch relationship, accounting for the pronounced increase in yield and tensile strengths at (830–850) °C.

The role of alloying elements, particularly Nb and Ti, should also be considered. These elements form fine carbides and carbonitrides (e.g., NbC, TiN) that pin grain boundaries and dislocations, further contributing to precipitation strengthening. During annealing, the dissolution and reprecipitation of these phases are temperature-dependent, influencing both recrystallization kinetics and final mechanical properties. At the highest annealing temperature (850 °C), a greater fraction of these precipitates may dissolve, but upon cooling they re-precipitate in a fine dispersion, enhancing strength while slightly reducing ductility.

The yield-to-tensile ratio (Y/T) increases monotonically with annealing temperature, reaching 0.82 at 850 °C. A high Y/T ratio indicates limited work-hardening capacity but excellent dimensional stability under load, a desirable characteristic for precision components such as rail rods, where elastic deformation must be minimized to maintain actuation accuracy.

In summary, annealing at 850 °C produces an optimal microstructure for the present application: a fine, homogeneous ferrite grain structure strengthened by grain refinement and precipitation, offering a balanced combination of high strength, sufficient ductility, and good structural stability.

5. Conclusions

Based on a systematic investigation of annealing temperatures ranging from 640 °C to 850 °C, the following conclusions are drawn regarding the microstructure and mechanical properties of T4003 ferritic stainless steel for pipe organ rail rod applications:

1. For long-term dimensional stability under cyclic loads, a fine and uniform ferritic microstructure is essential. Annealing at 850 °C facilitates complete recrystallization and a full $\gamma \rightarrow \alpha$ transformation, producing such a homogeneous grain structure. This refined microstructure is critical for rail rods to maintain precise alignment and consistent mechanical response over decades of service, minimizing drift and ensuring reliable actuation.
2. A balance between static strength and retained ductility is required to withstand both operational stresses and potential overloads. While annealing at 850 °C achieves the highest strength (yield strength of 508 MPa, tensile strength of 614 MPa), the associated moderate ductility provides a necessary safety margin against brittle fracture. This combination ensures that the rail rod can bear high static loads from the mechanism while tolerating occasional unintended forces without failure.
3. A high yield-to-tensile ratio (0.82 at 850 °C) is directly beneficial for precision control. This elevated ratio indicates superior dimensional stability under load and a narrow elastic-to-plastic transition, which translates to a more predictable and linear force-displacement relationship in the rail rod. This characteristic is paramount for preserving the precise touch and responsive feel of the organ keyboard, as it minimizes non-elastic deformation during play.

Therefore, annealing at 850 °C is established as the optimal heat treatment parameter for T4003 stainless steel, as it delivers the specific microstructural and mechanical profile that best meets the demanding requirements of reliability, durability, and precision in pipe organ rail rod mechanisms.

References

- [1] A. C. Disley and D. M. Howard, "The significance of relative loudness in listener identification of pipe organ stops," *J. Acoust. Soc. Am.*, vol. 120, no. 5, p. 3341, 2006, <https://doi.org/10.1121/1.4781338>
- [2] C. R. Smith, "From one pianist to another: The importance of organ playing," *American Music Teacher*, vol. 71, no. 1, pp. 18–21, 2021. [Online]. Available: <https://www.jstor.org/stable/27143461>
- [3] S. Zhao, "Tone recognition database of electronic pipe organ based on artificial intelligence," *Math. Problems Eng.*, vol. 2021, Art. no. 5526517, 2021, <https://doi.org/10.1155/2021/5526517>
- [4] B. Y. Kinzey Jr., "Preliminary observations of the influence of casework of pipe organs on room acoustical fields," *J. Acoust. Soc. Am.*, vol. 74, no. S1, p. S114, 2005, <https://doi.org/10.1121/1.2020759>
- [5] J. Zhang et al., "Precipitation and growth mechanism of TiN on Y₂O₃ (110) and (100) surfaces of yttrium-containing T4003 stainless steel," *Physica B: Condensed Matter*, vol. 684, Art. no. 415980, 2024, <https://doi.org/10.1016/j.physb.2024.415980>
- [6] Z. Zhang et al., "Microstructure evolution in heat affected zone of T4003 ferritic stainless steel," *Mater. Des.*, vol. 68, pp. 114–120, 2015, <https://doi.org/10.1016/j.matdes.2014.12.018>
- [7] Z. Li et al., "Microstructures and mechanical properties of hot-rolled and annealed Al–27%Si alloy strips," *J. Mater. Sci.: Mater. Electron.*, vol. 36, no. 22, 2025, <https://doi.org/10.1007/S10854-025-15448-W>
- [8] C. Lai et al., "Effect of cold-rolling reduction and isothermal annealing temperature on the recrystallization kinetics of 3005 aluminum alloy sheets," *J. Phys.: Conf. Ser.*, vol. 3080, no. 1, Art. no. 012194, 2025, <https://doi.org/10.1088/1742-6596/3080/1/012194>
- [9] T. Das et al., "Mechanical and microstructural properties of laser direct energy deposited 15–5 PH and SS 316L stainless steel," *Mater. Today: Proc.*, vol. 66, no. 9, pp. 3809–3813, 2022, <https://doi.org/10.1016/j.matpr.2022.06.249>
- [10] H. Jian et al., "Influence of annealing temperature on the microstructure and properties of large deformation 2024 aluminum alloy," *Metallogr. Microstruct. Anal.*, pp. 1–12, 2025, <https://doi.org/10.1007/S13632-025-01238-7>
- [11] X. D. Nong and X. L. Zhou, "Effect of scanning strategy on the microstructure, texture, and mechanical properties of 15–5PH stainless steel processed by selective laser melting," *Mater. Charact.*, vol. 174, Art. no. 111012, 2021, <https://doi.org/10.1016/j.matchar.2021.111012>
- [12] D. Y. Kwon et al., "Effect of annealing temperature on tensile and impact properties of S31803 duplex stainless steel," *Mater. Sci. Eng. A*, vol. 931, Art. no. 148222, 2025, <https://doi.org/10.1016/j.msea.2025.148222>
- [13] Institute of Advanced Materials and Technology, Univ. of Sci. and Technol. Beijing, et al., "Influence of the aging time on the microstructure and electrochemical behaviour of a 15–5PH ultra-high strength stainless steel," *Corros. Sci.*, vol. 139, pp. 185–196, 2018, <https://doi.org/10.1016/j.corsci.2018.04.032>
- [14] B. Zhang et al., "Microstructure and mechanical properties of high-efficiency laser-directed energy deposited 15–5PH stainless steel," *Mater. Charact.*, vol. 190, Art. no. 112080, 2022, <https://doi.org/10.1016/j.matchar.2022.112080>
- [15] P. Chootapa, S. Wiriyaart, and S. Kaewluan, "Effect of annealing temperature on the microstructural and mechanical properties of wire rod steel annealed using a biomass gasifier," *Energies*, vol. 18, no. 8, Art. no. 1912, 2025, <https://doi.org/10.3390/en18081912>
- [16] W. Chen et al., "Effect of heat treatment on microstructure and performances of additively manufactured 15–5PH stainless steel," *Opt. Laser Technol.*, vol. 157, Art. no. 108711, 2023, <https://doi.org/10.1016/j.optlastec.2022.108711>
- [17] Loyola Marymount University et al., "Effect of heat treatment on microstructure and mechanical properties of 15–5PH stainless steel for fastener applications," *Diffus. Found.*, vol. 22, pp. 118–139, 2019, <https://doi.org/10.4028/www.scientific.net/DF.22.118>
- [18] N. Khanna et al., "Experimental investigation and sustainability assessment to evaluate environmentally clean machining of 15–5PH stainless steel," *J. Manuf. Process.*, vol. 56, pp. 1027–1038, 2020, <https://doi.org/10.1016/j.jmapro.2020.05.016>
- [19] R. Ruslan et al., "The influence of annealing temperature on the grain size of a nickel metal catalyst suitable for carbon nanotube growth," *J. Phys.: Conf. Ser.*, vol. 2980, no. 1, Art. no. 012002, 2025, <https://doi.org/10.1088/1742-6596/2980/1/012002>
- [20] P. Liu et al., "Influence of surface ultrasonic rolling on microstructure and corrosion property of T4003 ferritic stainless steel welded joint," *Metals*, vol. 10, no. 8, Art. no. 1081, 2020, <https://doi.org/10.3390/met10081081>